Molecular Vision 2019; 25:93-105 <http://www.molvis.org/molvis/v25/93>
Received 4 October 2018 | Accepted 6 February 2019 | Published 8 February 2019

Primary closed angle glaucoma in the Basset Hound: Genetic investigations using genome-wide association and RNA sequencing strategies

James A.C. Oliver,[1] Sally L. Ricketts,[1] Markus H. Kuehn,[2] Cathryn S. Mellersh[1]

[1]Canine Genetics Research Group, Kennel Club Genetics Centre, Animal Health Trust, Lanwades Park, Kentford, Newmarket, Suffolk, United Kingdom; [2]The University of Iowa, Department of Ophthalmology and Visual Sciences, Iowa City, IO

Purpose: To investigate the genetic basis of primary closed angle glaucoma (PCAG) in European Basset Hounds using genome-wide association and RNA sequencing strategies.
Methods: DNA samples from 119 European Basset Hounds were genotyped on the 170 K SNP CanineHD BeadChip array (Illumina) comprising 37 with normal iridocorneal angles (controls), 57 with pectinate ligament abnormality (PLA cases), and 25 with PCAG (PCAG cases). Genome-wide association studies (GWASs) of the PLA and PCAG cases were conducted. Whole transcriptome sequences of iridocorneal angle tissues from five Basset Hounds with PCAG were compared with those from four dogs with normal eyes to investigate differences in gene expression between the affected and unaffected eyes in GWAS-associated loci. A variant in *NEB*, previously reported to be associated with PCAG in American Basset Hounds, was genotyped in cohorts of European Basset Hounds and non-Basset Hounds.
Results: The GWASs revealed 1.4 and 0.2 Mb regions, on chromosomes 24 and 37, respectively, that are statistically associated with PCAG. The former locus has previously been associated with glaucoma in humans. Whole transcriptome analysis revealed differential gene expression of eight genes within these two loci. The *NEB* variant was not associated with PLA or PCAG in this set of European Basset Hounds.
Conclusions: We identified two novel loci for canine PCAG. Further investigation is required to elucidate candidate variants that underlie canine PCAG.

Canine glaucoma is a heterogeneous group of neurodegenerative diseases that lead to progressive retinal ganglion cell death, optic nerve degeneration, and visual field deficits. Intraocular pressure (IOP) is a consistent risk factor for the development of canine glaucoma [1]. Glaucoma is described as primary if it occurs in the absence of an antecedent ocular disease process, such as intraocular inflammation, neoplasia, or lens instability [2]. Primary glaucoma is thought to be caused by unidentifiable and inherent abnormalities in the aqueous humor outflow apparatus of the eye and in adult dogs is further subdivided into primary open angle glaucoma (POAG) and primary closed angle glaucoma (PCAG) based on the appearance of the iridocorneal angle (ICA). In POAG, the IOP is usually pathologically elevated, even in the presence of an open ICA and normal pectinate ligament anatomy in the early disease stages [3]. PCAG, however, is associated with pectinate ligament abnormality (PLA), a form of goniodysgenesis, in several dog breeds [4-10]. PLA describes the broad sheets of tissue that span the ICA and is associated with increasing age [11-14]. Although PLA appears to be required, but not sufficient, for the development of PCAG, only a small fraction of dogs with PLA develop PCAG [15,16].

The increased prevalence of primary glaucoma in certain dog breeds implies a genetic etiology. The Basset Hound (BH) is a dog breed known to be affected by POAG and PCAG [4,17]. In common with three other canine breeds, POAG in the BH is an autosomal recessive trait due to a mutation in *ADAMTS17* (Gene ID 170691, OMIM 607511) [17-20]. PCAG, however, is thought to be complex and caused by multiple genetic and environmental factors [21-23]. Two previous studies of the genetics of PCAG have been reported in the American BH. A genome-wide association study (GWAS) of 37 PCAG cases and 41 controls revealed associations at two novel loci that contain the candidate genes *COL1A2* (Gene ID 1278, OMIM 120160) and *RAB22A* (GENE ID 57403, OMIM 612966), but no candidate variants were reported [22]. In a subsequent paper, the same group reported a non-synonymous variant in *NEB* (Gene ID 4703, OMIM 161650) segregates with PCAG in the BH (BROADD2 chr19:55,885,214 A>G) [21]. *COL1A2* and *NEB* are promising candidate genes based on their functions. *COL1A2* encodes the pro-α2 chain of collagen type 1 which is an important component of the trabecular meshwork, and previous studies have implicated

Correspondence to: James AC Oliver, Canine Genetics Research Group, Kennel Club Genetics Centre, Animal Health Trust, Lanwades Park, Kentford, Newmarket, Suffolk, United Kingdom; Phone: +44 (0)1638 751000; FAX: +44 (0)1638 555666; email: James.Oliver@aht.org.uk

the role of collagen genes in the pathogenesis of human primary glaucoma [24-28]. *NEB* encodes the muscle contractility regulating protein, nebulin, which is expressed in the ciliary body musculature, and the belief that muscle-related mechanisms are involved in the aqueous humor outflow pathways makes *NEB* a feasible candidate [21,29,30]. *RAB22A* is known to be an oncogene, and thus, this gene's potential role in primary glaucoma is more difficult to explain [31].

In this study, we investigated the genetic basis of PLA and PCAG in the European BH. First, we tested for a possible association between the reported *NEB* variant and PLA and PCAG. Second, we used a GWAS to identify loci associated with PLA or PCAG and then used an additional cohort of American BHs with PCAG to further evaluate statistically significant associations. We used RNA sequencing (RNA-Seq) to investigate differential gene expression and identify candidate genes in the GWAS-derived loci.

METHODS

Genotyping of the NEB variant: The *NEB* variant (BROADD2 chr19:55,885,214 A>G) reported by Ahram et al. [21] was genotyped in a cohort of 158 BHs (10 PCAG cases, 52 PLA cases, and 96 controls) and 83 non-BH dogs, comprising 31 different breeds, with Sanger sequencing using primers detailed in Table 1. The non-BH dogs formed part of a multi-breed screening panel that was created before the inception of this study. These dogs had not undergone previous ophthalmological examination.

Genome-wide association study: All DNA samples from privately owned pet dogs were collected following fully informed and written owner consent and with approval from the Animal Health Trust's Research and Ethical Committee (approval number 36–2016). This study was performed in accordance with the ARVO Statement for Use of Animals in Research. DNA samples from American PCAG dogs were provided by one of the coauthors (MK) and included members of a PCAG colony and client-owned dogs all originating within the USA. Dogs were designated as controls or PLA cases based on the results of gonioscopy performed by the primary author (JO), a board-certified veterinary ophthalmologist, and as previously described [12-14,32]. Dogs were designated as PCAG cases following examination by JO and other board-certified veterinary ophthalmologists. The inclusion criteria for the controls, PLA cases, and PCAG cases were as follows:

1. Controls: Dogs with normal appearing ICAs aged five years and older.

2. PLA cases: Dogs with PLA affecting at least 50% of the ICA of each eye. The controls and the PLA cases had IOP within normal limits and normal optic nerve head anatomy as assessed with direct and indirect ophthalmoscopy.

3. PCAG cases: Dogs with one eye with IOP >50 mmHg (arbitrary cutoff) without any possible cause of secondary glaucoma and the finding of severe PLA (>90% of the ICA affected) in the contralateral eye. No diagnostic techniques were performed on the affected eye to confirm closure of the ICA or to assess the pathology of the optic nerve head.

DNA for the GWAS was extracted from buccal mucosal swabs as previously described [17]. Only dogs clear of the published BH POAG mutation were used [17]. DNA samples were submitted at a concentration of 20 ng/µl and a volume of 25 µl to an external laboratory (Neogen; Lansing, MI) for genotyping on the CanineHD BeadChip (Illumina; San Diego, CA) which contains 172,115 single nucleotide polymorphisms (SNPs) [33]. The GWAS data were analyzed using the freely available software package PLINK [34]. Data were filtered for quality control parameters, including the sample call rate, SNP call rate, and minor allele frequency (MAF). SNPs were excluded from analysis if they had a MAF <0.05 or had a call rate of <97%. Individuals were excluded if >10% SNP genotypes were missing. GWASs were conducted using a standard unadjusted allelic chi-square test for association (1 degree of freedom (df)). Inflation of observed statistics due to relatedness or the population substructure was estimated with genomic control (λ). Data were subsequently corrected for population stratification using a mixed model in the freely available software GEMMA [35]. Five case and control GWASs were performed as detailed in Table 2. The p values for each SNP derived from the GWAS using GEMMA were used to create a Manhattan plot for each analysis. A p value of 0.05 after correction for multiple testing using the Bonferroni correction (0.05/number of tests) was the threshold

Table 1. Primer details used for Sanger sequencing of the *NEB* variant.

Genomic coordinate of *NEB* variant (CanFam2)	Forward primer sequence Reverse primer sequence	Amplicon size (bp)	Annealing temp (°C)
chr19:55,885,214	ACCAGTAAGGTGAGTGCTTTCC AGGCTATGATCTCAGAACTGATGC	103	57

Table 2. Summary of number of dogs, results of quality control filtering steps and correction of population stratification for the five GWAS analyses.

Analysis	Phenotype of cases	Phenotype of controls	No. cases	No. controls	SNPs with MAF <0.05	SNPs with <0.97 call rate	SNPs remaining for analysis	λ before correction	λ after correction	P value
1	PCAG	Controls	24	37	71,687	11,749	96,259	1.96	1.04	1.7×10^{-4}
2	PCAG + PLA	Controls	81	37	71,633	10,166	97,282	1.34	1.00	7.7×10^{-5}
3	PLA	Controls	57	37	73,253	11,935	94,781	1.28	1.01	1.0×10^{-4}
4	PCAG	PLA	24	57	72,150	9,858	96,868	2.23	1.01	$3.8\times10^{-7*}$
5	PCAG	Controls + PLA	24	94	71,633	10,166	97,282	2.25	0.96	$1.4\times10^{-7*}$

No.=number, λ=lambda (genomic inflation factor), * denotes significant association (Bonferonni)

for statistical association in all studies ($p<5.28 \times 10^{-7}$) and prompted further investigation of the associated loci. Associations between the GWAS SNPs and disease in individual dog data sets were assessed using logistic regression using an additive per allele model to compute an odds ratio and confidence interval for the association of one or more SNPs with disease using STATA 10.0 (College Station, TX).

Definition of associated loci: Associated loci were defined based on pairwise linkage disequilibrium (LD) estimates (conservative $r^2 \geq 0.5$) of the SNPs using the Tagger program embedded in Haploview [36,37]. A list of SNPs in LD with the most strongly associated GWAS SNP for each locus was generated which could denote a region tagged by the GWAS association signal. As for the GWAS, SNPs were excluded from analysis if they had a MAF <0.05 or a call rate of <97%.

Gene expression using RNA-Seq: Eyes were removed from five BHs with PCAG on welfare grounds and from four non-BH dogs with normal eyes that had been euthanized via intravenous overdose of pentobarbitone for reasons unrelated to this study. Following enucleation, each globe was transected along the sagittal plane into two equal halves. Each half globe was immersed in 15 ml RNA*later* solution (Ambion; Foster City, CA) before being stored at −80 °C until later use as previously described [38,39]. RNA was extracted from selected tissue samples using the Qiagen RNAeasy Midi Kit (Qiagen; Hilden, Germany) according to the manufacturer's instructions. Following thawing of each half globe, a section of the ICA was dissected under an operating microscope with microsurgical instrumentation aiming for approximately 200–250 mg tissue. The posterior boundary of the dissected tissue was the posterior pars plana, and the anterior boundary was the corneoscleral limbus. No lens tissue was included in the dissection, but the sclera was included. Adherent conjunctiva and episcleral tissues were removed. Total RNA (20 ng–1 µg per sample, at a concentration of ≥20 ng/µl with RNA integrity number (RIN) ≥8.0 and optical density (OD)260/280 ≥1.8) was submitted to Otogenetics Corporation (Atlanta, GA) for library preparation and sequencing: 1–2 µg of cDNA was generated using the Clontech Smart cDNA kit (Clontech Laboratories; Mountain View, CA) from 100 ng of total RNA. cDNA was fragmented using Covaris (Covaris; Woburn, MA) and profiled using an Agilent Bioanalyzer 2100 (Agilent; Santa Clara, CA). Libraries were prepared using NEBNext reagents (Catalog No. 634,925. New England Biolabs; Ipswich, MA): mRNAs were purified using Poly(A) selection from the total RNA sample and then fragmented. cDNA was then synthesized using random priming, followed by end repair, phosphorylation, A-tailing, adaptor ligation, and finally, PCR amplification. The quality, quantity, and size distribution of the Illumina libraries were determined using an Agilent Bioanalyzer 2100. The libraries were then loaded on an Illumina HiSeq2500 for clustering and sequencing according to the standard operation. Paired-end 90–100 nucleotide reads were generated, and data quality was assessed using FASTQC (Babraham Institute; Cambridge, UK). After optimum quality control (QC) results were achieved, the samples were analyzed. Sequence reads (minimum of 50 M per sample) were mapped to the CanFam3.1 reference genome, and the read count values of gene expression (fragments per kilobase million, FPKM) were calculated. The differential expression of the FPKM (the read counts) between the PCAG cases and controls was calculated as the base 2 log of the fold change of controls/PCAG cases ($\log_2$ (the FPKM of the PCAG cases/the FPKM of the controls)). The test statistic was used to compute the statistical significance of the observed change in the FPKM. The p value represents the uncorrected p value of the test statistic, and the Q value represents the false discovery rate–adjusted p value of the test statistic. For genes shown to be differentially expressed, their functions and associated

phenotypes (for potential candidacy for canine PCAG) were assessed using VarElect GeneCards®.

RESULTS

NEB variant genotyping: One hundred fifty-seven BHs (ten PCAG cases, 52 PLA cases, and 95 controls) were homozygous for the reported *NEB* variant (G/G), and only one control was heterozygous (A/G). In the 83 non-BH dogs, 59 were homozygous for the variant (G/G), 15 were heterozygous (A/G), and only nine were homozygous for the reference allele (A/A). Thus, as well as not being associated with PLA or PCAG, it appeared that the SNP at this location is a common polymorphism, and the reported variant may actually be more common in European dogs than the reference allele.

Genome-wide association studies: The results of the five GWASs, including case and control designation, filtering steps, the genomic inflation factor, and the p value of the top SNP from each analysis can be found in Table 2. Statistically significant SNP associations were found in GWAS Analyses 4 and 5. In Analysis 4 (Cases: PCAG cases; Controls: PLA cases), a SNP on canine chromosome 24 (BICF2G630505097; CanFam3.1 chr24:17,381,226; $p = 3.8 \times 10^{-7}$) reached the threshold of genome-wide statistical association (Figure 1). In Analysis 5 (Cases: PCAG cases; Controls: PLA cases and control dogs), an additional SNP in the same region increased the strength of the statistical association further (BICF2P544799; CanFam3.1 chr24:18,739,902; $p = 1.4 \times 10^{-7}$; Figure 2).

GWAS conditioning on the most strongly associated SNP was performed to assess whether any additional loci were associated with PCAG. To achieve this, SNP BICF2P544799 was introduced as a covariate in the mixed model in Analysis 5. This revealed an additional SNP at a distinct chromosomal location on canine chromosome 37 to reach the threshold of genome-wide statistical association (BICF2P928441; CanFam3.1 chr37: 24,747,131; $p = 1.9 \times 10^{-7}$; Figure 3). Conditional analysis using both associated SNPs as covariates in the model revealed no further association signals.

The interrelationships between the three strongest associated SNPs and PCAG risk were further assessed in the individual SNP data sets using logistic regression. This was done for the original GWAS set and with the addition of PCAG cases from the USA. All three SNPs were strongly associated with PCAG, and the strength of association increased following the addition of the American dogs with PCAG to the analyses (Table 3). A combined analysis of the two SNPs and the risk of PCAG in all 153 dogs (59 cases and 94 controls defined as Table 3) using an additive (per allele) model resulted in an odds ratio of 19.30 (95% confidence interval 7.62–48.85; $p = 1.4 \times 10^{-24}$).

Definition of associated loci: A critical region spanning the top associated SNPs was defined based on pairwise LD of these top three SNPs with other SNPs on the respective chromosome in the GWAS data set. Although the top two chromosome 24 SNPs BICF2G630505097 and BICF2P544799 were correlated at an r^2 of 0.79 in this study set, they were both

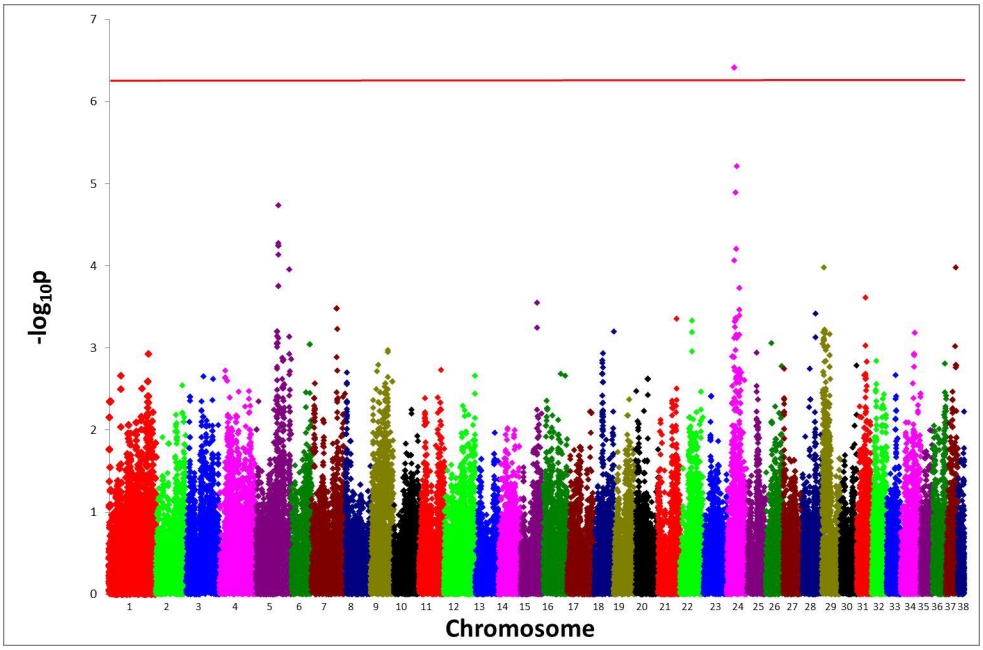

Figure 1. Manhattan plot for GWAS Analysis 4 (Cases: PCAG cases; Controls: PLA cases) in the European BH. The horizontal red line denotes the threshold for genome-wide statistical association.

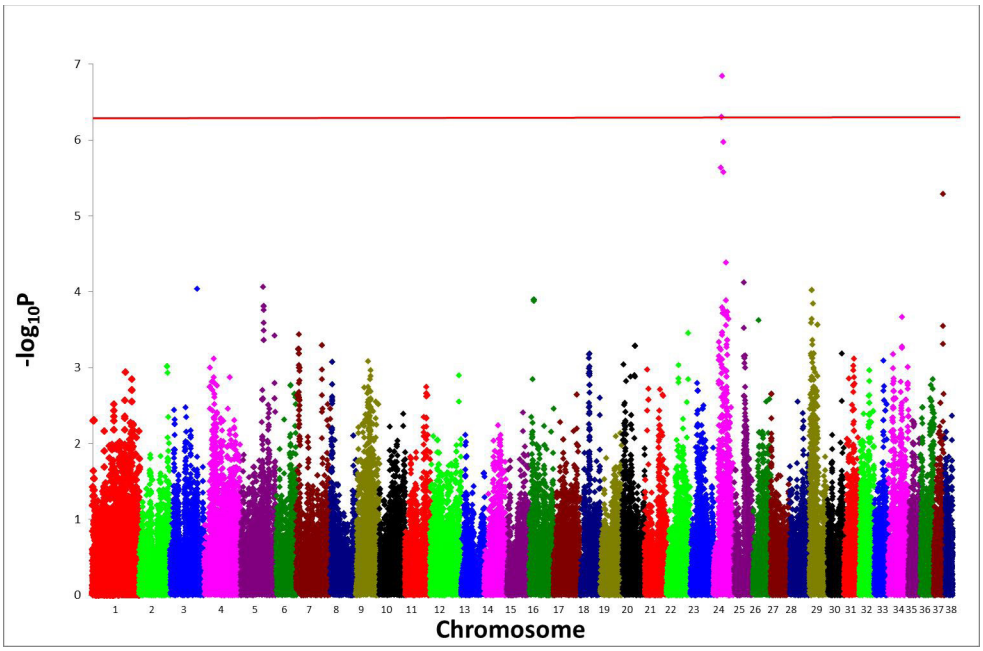

Figure 2. Manhattan plot for GWAS Analysis 5 (Cases: PCAG cases; Controls: PLA cases and control dogs) in the European BH. The horizontal red line denotes the threshold for genome-wide statistical association.

used as tag SNPs to ensure coverage. From these analyses, the following chromosomal loci were defined for subsequent investigation: CanFam3.1 chr24:17,381,226–18,739,902 and chr37:24,747,131–24,958,250.

Identification of candidate genes from RNA-Seq: Whole transcriptome data derived from ICA tissues were used to compare differential gene expression between BH PCAG cases (n=5) and non-BH controls (n=4) in the extended loci determined from GWAS and LD analysis (Table 4). In the chromosome 24 locus, differential gene expression was present for five genes or loci: *SIGLEC1* (Gene ID 6614, OMIM 600751), C24H20orf194, *SLC4A11* (Gene ID 83959, OMIM 610206), *PROSAPIP1* (Gene ID 9762, OMIM 610484), and *OXT* (Gene ID 5020, OMIM 167050). In the chromosome 37 locus, differential expression was present for three genes: *CXCR2* (Gene ID 3579, OMIM 146928), *CXCR1* (Gene ID

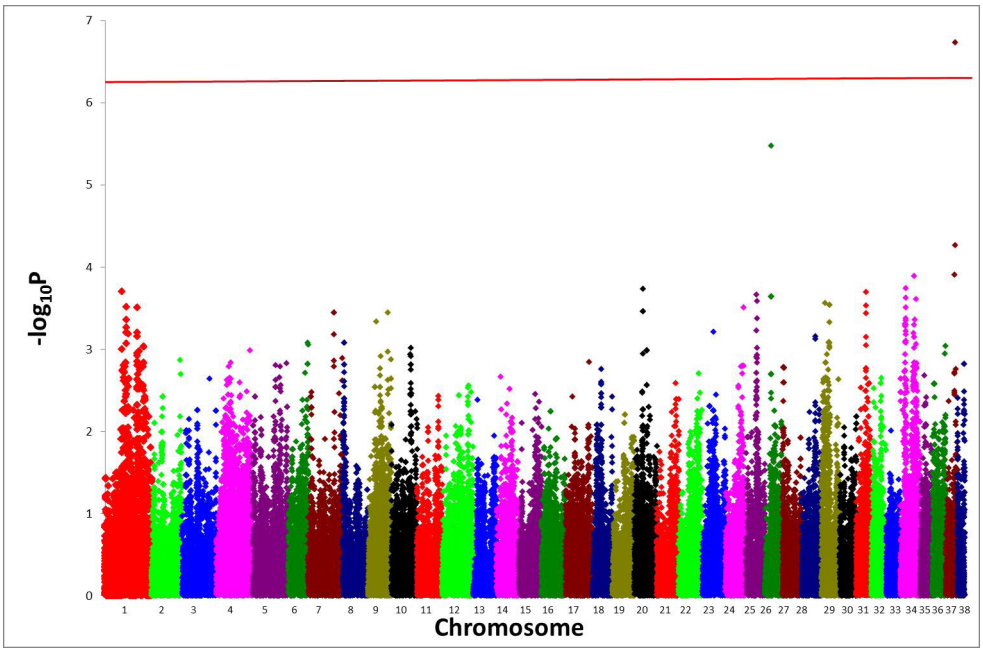

Figure 3. Manhattan plot for GWAS analysis 5 (Cases: PCAG cases; Controls: PLA cases and control dogs) in the European BH using BICF2P544799 as a covariate. The horizontal red line denotes the threshold for genome-wide statistical association.

3577, OMIM 146929) and *ARPC2* (Gene ID 10109, OMIM 604224). A survey of the functions and associated phenotypes of these genes revealed no evidence of reported association with glaucoma. All genes, however, appear to be involved in inflammation or immunity (Table 5).

DISCUSSION

Canine PCAG is considered complex, likely involving multiple genetic and environmental factors [40]. GWASs have been used extensively in the human field over the last two decades to improve the understanding of the genetic basis of many complex traits by revealing associated susceptibility loci and have provided invaluable insights into the allelic architecture of many multifactorial traits [41]. In humans, GWASs of thousands of individuals are usually required to find significant associations with complex diseases [42,43]. More recently, findings from human GWASs of complex disease have supported the original hypothesis that their genetic architecture is mainly comprised of common variants with modest or intermediate effect, as well as a smaller subset of high-penetrant (familial) low-frequency variants of high effect [44]. In the dog, however, many fewer canine samples are required to detect a statistically significant association compared to human studies, owing to the more limited genomic architecture and haplotype structure of domestic dog breeds [22,23,45-47]. In the present GWAS, a locus on canine chromosome 24 was found to be associated with PCAG relative to PLA in Analysis 4 using a total of only 81 dogs (24 PCAG cases and 57 PLA cases), and the level of statistical association was further increased when the controls were combined with the PLA cases in Analysis 5 (a total of 118 dogs). An additional locus was found on canine chromosome 37 following conditional analysis. Owing to our employment of correction for population stratification and the stringent threshold for a statistically significant association, it is unlikely that these are false positive associations [48]; in addition, the strength of the associations was augmented by the addition of the American BH PCAG cases. This was particularly marked for BICF2G630505097 which was also the most strongly associated SNP in GWAS Analysis 4 (Cases: PCAG cases; Controls: PLA cases). This SNP is located in an intergenic region (chr24:17,381,226) with *RNF24* (Gene ID 11237, OMIM 612489; chr24:17,423,245–17,454,478) and *PANK2* (Gene ID 80025, OMIM 606157; chr24:17,463,603–17,489,677) the nearest upstream genes. These genes may prove to be candidate genes for PCAG as a previous study of a glaucoma-related trait in humans, optic nerve head morphology, revealed a statistically significant linkage signal at the RNF24/PANK2 locus [49].

The present GWAS results did not corroborate those of previous studies in the BH. A GWAS of PCAG in American BHs reported two regions were associated with PCAG [22]. These susceptibility loci were situated on canine chromosomes 14 and 24 (chr14:19,911,001–20,161,358 and chr24:43,091,222–43,595,979) and contained the collagen gene *COL1A2* and oncogene *RAB22A,* respectively. The inability to reproduce these findings in the present GWAS might be related to population differences in the frequency of the risk loci between European BHs and American BHs. Another study in American BHs by the same investigators used linkage analysis followed by exome-sequencing analysis to identify an SNP in *NEB* to segregate with PCAG [21]. The present study, however, did not find any association between this variant and PCAG, and the multibreed genotyping suggested that this variant is a common polymorphism. As the resequencing study that identified this *NEB* variant captured only the exome, it is possible that the variant is tagging a true functional variant underlying the linkage study results [21]. However, although a recessive mode of inheritance was assumed, the logarithm (base 10) of odds (LOD) score was considerably lower than those achieved for other recessive diseases that have been mapped in a similar

Table 3. Association of GWAS top SNPs with PCAG in the BH (Analysis 5 (see Table 2)

Top SNP from GWAS	USA PCAG cases included?	No. PCAG cases	No. PLA cases and controls	OR	Lower 95% CI	Upper 95% CI	P-value
chr24:17381226 BICF2G630505097	No	24	94	13.73	5.06	37.26	4.2×10^{-11}
	Yes	59	94	18.84	7.97	44.51	1.6×10^{-21}
chr24:18739902 BICF2P544799	No	24	94	28.35	8.50	94.58	1.6×10^{-11}
	Yes	59	94	15.81	6.03	41.45	1.4×10^{-12}
chr37: 24,747,131 BICF2P928441	No	24	94	18.03	4.44	73.28	1.1×10^{-6}
	Yes	59	94	14.76	4.19	51.96	3.6×10^{-8}

No.=number, OR=odds ratio, CI=confidence interval

Table 4. Differential gene expression results for the BH PCAG loci.

Gene	CanFam3.1 coordinate	Status	FPKM Controls	FPKM PCAG cases	log_2(fold change)	Test statistic	P-value	Q-value	Signifi-cant?
Locus chr24:17,381,226–18,739,902									
LOC100855425	24:17377802–17459234	OK	3.66177	4.27275	0.222624	0.105002	0.90045	0.972499	no
RNF24	24:17377802–17459234	OK	13.5062	15.8018	0.226461	0.549112	0.2461	0.564651	no
PAX1	24:1743907–1752578	NOTEST	0.751058	0.206085	−1.86569	0	1	1	no
PANK2	24:17463086–17489560	OK	19.9698	18.2754	−0.127921	−0.289163	0.55265	0.833548	no
MAVS	24:17511842–17529197	OK	29.2054	32.6664	0.161573	0.390852	0.42265	0.743935	no
AP5S1	24:17539786–17543605	OK	8.54101	8.52501	−0.00270593	−0.00393991	0.99425	0.998863	no
CDC25B	24:17552205–17561823	OK	12.1744	14.8	0.28175	0.556191	0.2447	0.563837	no
CENPB	24:17569396–17572311	OK	31.9742	38.916	0.283456	0.799702	0.1328	0.393219	no
SPEF1	24:17572374–17578571	OK	1.5338	1.92433	0.327243	0.400218	0.3999	0.724145	no
C24H20orf27	24:17586019–17600147	OK	22.4481	29.0792	0.373394	0.779776	0.1107	0.352522	no
HSPA12B	24:17600534–17619889	OK	6.57984	9.70452	0.560605	1.14769	0.0296	0.142427	no
SIGLEC1	24:17636164–17667080	OK	2.18752	12.5593	2.52139	4.87528	5.00E-05	0.0008345	yes
ADAM33	24:17668462–17682217	OK	10.7869	8.23265	−0.389845	−0.829875	0.0807	0.285699	no
GFRA4	24:17686816–17690747	OK	3.16594	2.14218	−0.563553	−0.711984	0.2384	0.555935	no
ATRN	24:17698237–17859816	OK	18.7085	14.7908	−0.338994	−0.812765	0.08165	0.288073	no
C24H20orf194	24:17908366–18050002	OK	14.0202	9.25396	−0.599364	−1.46229	0.00165	0.0153647	yes
SLC4A11	24:18057411–18068425	OK	28.8724	6.6876	−2.11013	−4.36281	5.00E-05	0.0008345	yes
ITPA	24:18070979–18082187	OK	11.9247	16.3186	0.452557	0.814939	0.0945	0.316902	no
DDRGK1	24:18085722–18098868	OK	17.4284	15.1717	−0.200057	−0.450069	0.33115	0.659854	no
LOC102157332	24:18111855–18122295	NOTEST	0.531426	0.412288	−0.366218	0	1	1	no
PROSAPIP1	24:18111855–18122295	OK	20.0459	12.6993	−0.658565	−1.63743	0.00105	0.0107012	yes
FASTKD5	24:18124262–18166506	OK	13.9635	14.315	0.0358696	0.0772293	0.86905	0.965583	no
CST11	24:181590–184213	NOTEST	0	0	0	0	1	1	no
AVP	24:18183056–18184827	NOTEST	0.182349	0.0787568	−1.21123	0	1	1	no
OXT	24:18193380–18194236	OK	18.6151	5.43912	−1.77503	−2.94744	0.0006	0.0068551	yes
MRPS26	24:18215054–18217105	OK	24.9994	26.2617	0.0710653	0.176449	0.7648	0.934576	no
LOC102151131	24:18217903–18222755	NOTEST	0.0563875	0.0232463	−1.27838	0	1	1	no
LOC102154818	24:18224354–18395654	NOTEST	0.867838	0.884208	0.0269605	0	1	1	no
PTPRA	24:18224354–18395654	OK	30.9735	28.6433	−0.112839	−0.288467	0.5554	0.835146	no
VPS16	24:18401450–18424606	OK	11.5555	11.6659	0.0137143	0.0286225	0.95285	0.989023	no
PCED1A	24:18424775–18429698	OK	18.7163	16.9792	−0.140525	−0.340822	0.5442	0.828421	no

Molecular Vision 2019; 25:93-105 <http://www.molvis.org/molvis/v25/93>

Gene	CanFam3.1 coordinate	Status	FPKM Controls	FPKM PCAG cases	log_2(fold change)	Test statistic	P-value	Q-value	Signifi-cant?
LOC102155387	24:18442763–18443512	NOTEST	0.12029	0.206892	0.782359	0	1	1	no
TMEM239	24:18443575–18445637	NOTEST	0.308423	0.133061	−1.21283	0	1	1	no
C24H20orf141	24:18445693–18446873	NOTEST	0.202272	0.317907	0.652307	0	1	1	no
CPXM1	24:18453867–18460350	OK	8.40695	13.7502	0.7098	1.29913	0.0077	0.0506978	no
EBF4	24:18470596–18528305	OK	1.69066	1.6627	−0.0240522	−0.0278686	0.96215	0.991001	no
IDH3B	24:18556489–18561401	OK	46.7683	38.3285	−0.287114	−0.659815	0.1486	0.420704	no
NOP56	24:18561409–18566780	OK	28.0915	30.953	0.139945	0.325807	0.48615	0.78904	no
TMC2	24:18577342–18642204	NOTEST	0.308586	0.147869	−1.06136	0	1	1	no
ZNF343	24:18661008–18665685	NOTEST	0.245175	0.133892	−0.872746	0	1	1	no
SNRPB	24:18674022–18683315	OK	62.0096	61.9386	−0.00165212	−0.004023	0.99365	0.998542	no
TGM6	24:18700241–18721827	NOTEST	0.0171946	0	-	0	1	1	no
TGM3	24:18753637–18793790	NOTEST	0.0342808	0.138228	2.01158	0	1	1	no
Locus chr37:24,747,131–24,958,250									
RUFY4	37:24809358–24830254	OK	1.71109	1.18547	−0.52945	−0.51443	0.27475	0.599772	no
CXCR2	37:24831509–24846517	OK	3.35508	1.02764	−1.70702	−1.59836	0.00145	0.013826	yes
CXCR1	37:24861913–24866062	OK	1.82409	0.616257	−1.56557	−1.58159	0.0041	0.030963	yes
ARPC2	37:24914388–24936198	OK	84.4912	137.67	0.704343	1.97128	0.00035	0.004435	yes
GPBAR1	37:24940929–24943399	OK	1.26415	2.05007	0.697505	0.919835	0.14675	0.417894	no
AAMP	37:24943657–24948585	OK	40.9075	43.1513	0.077039	0.181187	0.70665	0.913414	no
PNKD	37:24948682–25008542	OK	6.30845	7.78033	0.302547	0.202254	0.70135	0.911242	no

OK=test successful, NOTEST=not enough alignments for testing

Molecular Vision 2019; 25:93-105 <http://www.molvis.org/molvis/v25/93>

© 2019 Molecular Vision

Table 5. Details of differentially expressed genes, their functions and associated disorders and phenotypes (assessed using VarElect GeneCards®)

Gene	Gene full name	Function	Associated disorders/ phenotypes
SIGLEC1	Sialoadhesin	Endocytic receptor mediating clathrin dependent endocytosis	Glomerulonephritis Sclerosis X-linked intellectual disability
C20orf194	Chromosome 20 open reading frame 194	May act as an effector for ARL3	HIV-1 Hepatitis
SLC4A11	Solute Carrier Family 4 Member 11	Transporter which plays an important role in sodium-mediated fluid transport in different organs.	Corneal dystrophy HIV-1 Hepatitis
PROSAPIP1	Proline Rich Synapse Associated Protein Interacting Protein 1	May be involved in promoting the maturation of dendritic spines	Hepatitis
OXT	Oxytocin	Contraction of smooth muscle of uterus and mammary gland	Persistent genital arousal Endometritis Inhibited male orgasm Epignathus Chorioamnionitis Parturition Lactation
CXCR1	Chemokine (CXC) Receptor 1	Neutrophil activation, neutrophil count	HIV-1 Pyelonephritis & urinary tract infections Idiopathic anterior uveitis
CXCR2	Chemokine (CXC) Receptor 2	Neutrophil activation, neutrophil count	Congenital neutropaenia Neutrophil migration Pyelonephritis Septicaemia Granulocytic anaplasmosis
ARPC2	Actin Related Protein 2/3 Complex Subunit 2	Actin filament assembly. Platelet, reticuloycte and neutrophil count	Platelet, reticuloycte and neutrophil count

way [21,50-52]. Therefore, it is possible that this result was a chance finding; the magnitude of associations identified in the present GWAS, which used stringent correction for multiple testing and a set of American BHs that validated the results, does not support PCAG in the BH to be a recessive disease from the sample set we analyzed; PCAG is more likely to be of complex etiology.

It was interesting that a statistically significant association of SNPs with PCAG was found in Analysis 4 (Cases: PCAG cases; Controls: PLA cases) and not in Analysis 2 (Cases: PCAG and PLA cases; Controls: control dogs). PLA is considered a consistent risk factor for, and therefore, likely to be on the causal pathway to, canine PCAG [5,9,15,53]. Thus, we considered it probable that there are shared genetic factors between PCAG and PLA cases, and a statistically significant association with disease (PCAG or PLA or both) would more likely be discovered when PCAG is analyzed combined with PLA cases against controls owing to the greater number of cases, and thus, power, of such analysis. Instead, these studies revealed two loci that are statistically significantly more common in PCAG cases than in PLA cases and controls. This is not a completely unexpected finding, however, as although PLA is a risk factor for PCAG, only a minority of dogs with PLA develop PCAG. This study supports the theory that PLA is *required* for but is not *sufficient* for PCAG. Thus, it is likely that the two chromosomal loci identified are involved in the trigger of the progression from PLA to PCAG. This finding will influence our ongoing investigations of the allelic architecture of PCAG in the BH. Future investigations to identify causal variants for PCAG in these loci will likely utilize a next-generation whole genome sequencing (WGS) approach using multiple PCAG and PLA

cases and subsequent genotyping of segregating variants in extended case-control sets. For complex disease, such as canine PCAG, a relatively large sample set is likely to be needed. Furthermore, the efficiency of a WGS approach will likely be improved by selecting dogs based on a homozygous genotype for the most strongly associated GWAS SNPs.

The main challenge of GWASs in investigating complex disease is to pinpoint possible causal variants underlying association signals as the majority of GWAS hits are in non-coding or intergenic regions because complex disease is often caused by disturbance to biologic networks, not by isolated genes or proteins [54]. Regulatory SNPs can influence gene expression through several mechanisms that include the three-dimensional organization of the genome, RNA splicing, transcription factor binding, DNA methylation, and long non-coding RNAs [55,56]. In an attempt to overcome these limitations, we used RNA-Seq. We first used the most strongly associated SNPs from the present GWASs to define chromosomal loci based on their ability to be tagged by other nearby SNPs. We then used RNA-Seq to compare gene expression between affected and unaffected dogs within these loci. Eight genes were found to be differentially expressed, and none of these genes are obvious candidates for canine PCAG. Instead, most of the genes identified have functions related to inflammation and immunity. This finding was not completely unexpected as the results of several other studies have implicated the role of inflammation and immunity in the pathogenesis of canine and human glaucoma [57-62]. Thus, the present results appear to corroborate these findings. However, intraocular inflammation may have occurred secondary to the onset of PCAG in the cases we used for RNA-Seq. Inflammation is a common histological finding in eyes affected by primary and secondary glaucoma, and there is no published evidence of inflammation being present in eyes considered at risk of PCAG (i.e., those with severe PLA) [63–65].

There are several study limitations that should be discussed. This GWAS included many fewer individuals compared to studies of complex disease in humans. In the dog, much more modest sample numbers are generally used mainly as a result of limitations in sample availability, robust phenotypic characterization, and funding. The limitations in sample availability in the present study also, unfortunately, meant it was not possible to repeat the GWAS with an additional replication set of samples. There were also limitations in the RNA-Seq investigations. The lack of ocular tissue from BHs with normal eyes meant that tissues from other breeds had to be used that represent sub-optimal control samples. Furthermore, the sequencing of RNA from multiple cell types that make up the ICA and neighboring structures could have led to a misleading pattern of differential gene expression than is actually occurring in the specific region of the ICA that is directly implicated in the pathogenesis of PCAG.

In conclusion, we successfully used GWASs to identify two novel loci associated with canine PCAG. Comparison of the gene expression profiles implicated genes involved in inflammation and immunity as involved in pathogenesis. WGS, involving multiple dogs, is likely required to elucidate candidate causal variants for canine PCAG that underlie the present GWAS findings.

ACKNOWLEDGMENTS

This work was supported by Dogs Trust, the European College of Veterinary Ophthalmologists (ECVO2017) and the Kennel Club. The authors would like to thank all the dog owners that allowed us to examine and collect samples from their dogs and also Prof. Hannes Lohi for contributing samples to the GWAS.

REFERENCES

1. Armaly MF, Krueger DE, Maunder L, Becker B, Hetherington J Jr, Kolker AE, Levene RZ, Maumenee AE, Pollack IP, Shaffer RN. Biostatistical analysis of the collaborative glaucoma study. I. Summary report of the risk factors for glaucomatous visual-field defects. Arch Ophthalmol 1980; 98:2163-71. [PMID: 7447768].
2. Pizzirani S. Definition, Classification, and Pathophysiology of Canine Glaucoma. Vet Clin North Am Small Anim Pract 2015; 45:1127-57. [PMID: 26456751].
3. Gelatt KN, Peiffer RL Jr, Gwin RM, Sauk JJ Jr. Glaucoma in the beagle. Trans Sect Ophthalmol Am Acad Ophthalmol Otolaryngol 1976; 81:Op636-44. [PMID: 960386].
4. Bedford P. A gonioscopic study of the iridocorneal angle in the English and Amercian breeds of Cocker Spaniel and Basset Hound. J Small Anim Pract 1977; 18:631-4. [PMID: 604666].
5. Bjerkås E, Ekesten B, Farstad W. Pectinate ligament dysplasia and narrowing of the iridocorneal angle associated with glaucoma in the English Springer Spaniel. Vet Ophthalmol 2002; 5:49-54. [PMID: 11940248].
6. Ekesten B, Narfstrom K. Age-related changes in intraocular pressure and iridocorneal angle in Samoyeds. Progress in Veterinary and Comparative Ophthalmology. 1992; 2:37-40. .
7. Ekesten B, Narfstrom K. Correlation of morphologic features of the iridocorneal angle to intraocular pressure in Samoyeds. Am J Vet Res 1991; 52:1875-8. [PMID: 1785731].
8. Fricker GV, Smith K, Gould DJ. Survey of the incidence of pectinate ligament dysplasia and glaucoma in the UK

Leonberger population. Vet Ophthalmol 2016; 19:379-85. [PMID: 26359130].

9. Read RA, Wood JL, Lakhani KH. Pectinate ligament dysplasia (PLD) and glaucoma in Flat Coated Retrievers. I. Objectives, technique and results of a PLD survey. Vet Ophthalmol 1998; 1:85-90. [PMID: 11397215].

10. Wood JL, Lakhani KH, Mason IK, Barnett KC. Relationship of the degree of goniodysgenesis and other ocular measurements to glaucoma in Great Danes. Am J Vet Res 2001; 62:1493-9. [PMID: 11560283].

11. Pearl R, Gould D, Spiess B. Progression of pectinate ligament dysplasia over time in two populations of Flat-Coated Retrievers. Vet Ophthalmol 2015; 18:6-12. [PMID: 24025050].

12. Oliver JA, Ekiri A, Mellersh CS. Prevalence of pectinate ligament dysplasia and associations with age, sex and intraocular pressure in the Basset hound, Flatcoated retriever and Dandie Dinmont terrier. Canine Genet Epidemiol 2016; 3:1-[PMID: 26973793].

13. Oliver JA, Ekiri A, Mellersh CS. Prevalence and progression of pectinate ligament dysplasia in the Welsh springer spaniel. J Small Anim Pract 2016; 57:416-21. [PMID: 27251455].

14. Oliver JA, Ekiri AB, Mellersh CS. Pectinate ligament dysplasia in the Border Collie, Hungarian Vizsla and Golden Retriever. Vet Rec 2017; 180:279-[PMID: 27999154].

15. Wood JL, Lakhani KH, Read RA. Pectinate ligament dysplasia and glaucoma in Flat Coated Retrievers. II. Assessment of prevalence and heritability. Vet Ophthalmol 1998; 1:91-9. [PMID: 11397216].

16. Miller PE, Bentley E. Clinical Signs and Diagnosis of the Canine Primary Glaucomas. Vet Clin North Am Small Anim Pract 2015; 45:1183-212. [PMID: 26456752].

17. Oliver JA, Forman OP, Pettitt L, Mellersh CS. Two Independent Mutations in ADAMTS17 Are Associated with Primary Open Angle Glaucoma in the Basset Hound and Basset Fauve de Bretagne Breeds of Dog. PLoS One 2015; 10:e0140436-[PMID: 26474315].

18. Forman OP, Pettitt L, Komaromy AM, Bedford P, Mellersh C. A Novel Genome-Wide Association Study Approach Using Genotyping by Exome Sequencing Leads to the Identification of a Primary Open Angle Glaucoma Associated Inversion Disrupting ADAMTS17. PLoS One 2015; 10:e0143546-[PMID: 26683476].

19. Oliver JAC, Rustidge S, Pettitt L, Jenkins CA, Farias FHG, Giuliano EA, Mellersh CS. Evaluation of ADAMTS17 in Chinese Shar-Pei with primary open-angle glaucoma, primary lens luxation, or both. Am J Vet Res 2018; 79:98-106. [PMID: 29287154].

20. Forman OP, De Risio L, Matiasek K, Platt S, Mellersh C. Spinocerebellar ataxia in the Italian Spinone dog is associated with an intronic GAA repeat expansion in ITPR1. Mamm Genome 2015; 26:108-17. [PMID: 25354648].

21. Ahram DF, Grozdanic SD, Kecova H, Henkes A, Collin RW, Kuehn MH. Variants in Nebulin (NEB) Are Linked to the Development of Familial Primary Angle Closure Glaucoma in Basset Hounds. PLoS One 2015; 10:e0126660-[PMID: 25938837].

22. Ahram DF, Cook AC, Kecova H, Grozdanic SD, Kuehn MH. Identification of genetic loci associated with primary angle-closure glaucoma in the basset hound. Mol Vis 2014; 20:497-510. [PMID: 24791135].

23. Ahonen SJ, Pietilä E, Mellersh CS, Tiira K, Hansen L, Johnson GS, Lohi H. Genome-wide association study identifies a novel canine glaucoma locus. PLoS One 2013; 8:e70903-[PMID: 23951034].

24. Zhou L, Higginbotham EJ, Yue BY. Effects of ascorbic acid on levels of fibronectin, laminin and collagen type 1 in bovine trabecular meshwork in organ culture. Curr Eye Res 1998; 17:211-7. [PMID: 9523101].

25. Wiggs JL, Howell GR, Linkroum K, Abdrabou W, Hodges E, Braine CE, Pasquale LR, Hannon GJ, Haines JL, John SW. Variations in COL15A1 and COL18A1 influence age of onset of primary open angle glaucoma. Clin Genet 2013; 84:167-74. [PMID: 23621901].

26. Shuai P, Yu M, Li X, Zhou Y, Liu X, Liu Y, Zhang D, Gong B. Genetic associations in PLEKHA7 and COL11A1 with primary angle closure glaucoma: a meta-analysis. Clin Experiment Ophthalmol 2015; 43:523-30. [PMID: 25732101].

27. Chen Y, Chen X, Wang L, Hughes G, Qian S, Sun X. Extended association study of PLEKHA7 and COL11A1 with primary angle closure glaucoma in a Han Chinese population. Invest Ophthalmol Vis Sci 2014; 55:3797-802. [PMID: 24854855].

28. Suri F, Yazdani S, Chapi M, Safari I, Rasooli P, Daftarian N, Jafarinasab MR, Ghasemi Firouzabadi S, Alehabib E, Darvish H, Klotzle B, Fan JB, Turk C, Elahi E. COL18A1 is a candidate eye iridocorneal angle closure gene in humans. Hum Mol Genet 2018; [PMID: 30007336].

29. Chu M, Gregorio CC, Pappas CT. Nebulin, a multi-functional giant. J Exp Biol 2016; 219:146-52. [PMID: 26792324].

30. Overby DR, Bertrand J, Schicht M, Paulsen F, Stamer WD, Lutjen-Drecoll E. The structure of the trabecular meshwork, its connections to the ciliary muscle, and the effect of pilocarpine on outflow facility in mice. Invest Ophthalmol Vis Sci 2014; 55:3727-36. [PMID: 24833737].

31. Zhang Y, Zhao FJ, Chen LL, Wang LQ, Nephew KP, Wu YL, Zhang S. MiR-373 targeting of the Rab22a oncogene suppresses tumor invasion and metastasis in ovarian cancer. Oncotarget 2014; 5:12291-303. [PMID: 25460499].

32. Oliver JAC, Cottrell BC, Newton JR, Mellersh CS. Gonioscopy in the dog: inter-examiner variability and the search for a grading scheme. J Small Anim Pract 2017; 58:652-658. [PMID: 28869290].

33. Vaysse A, Ratnakumar A, Derrien T, Axelsson E, Rosengren Pielberg G, Sigurdsson S, Fall T, Seppälä EH, Hansen MS, Lawley CT, Karlsson EK. LUPA Consortium. Bannasch D, Vilà C, Lohi H, Galibert F, Fredholm M, Häggström J, Hedhammar A, André C, Lindblad-Toh K, Hitte C, Webster MT. Identification of genomic regions associated with

phenotypic variation between dog breeds using selection mapping. PLoS Genet 2011; 7:e1002316-[PMID: 22022279].

34. Purcell S, Neale B, Todd-Brown K, Thomas L, Ferreira MA, Bender D, Maller J, Sklar P, de Bakker PI, Daly MJ, Sham PC. PLINK: a tool set for whole-genome association and population-based linkage analyses. Am J Hum Genet 2007; 81:559-75. [PMID: 17701901].

35. Zhou X, Stephens M. Genome-wide efficient mixed-model analysis for association studies. Nat Genet 2012; 44:821-4. [PMID: 22706312].

36. Barrett JC, Fry B, Maller J, Daly MJ. Haploview: analysis and visualization of LD and haplotype maps. Bioinformatics 2005; 21:263-5. [PMID: 15297300].

37. de Bakker PI, Yelensky R, Pe'er I, Gabriel SB, Daly MJ, Altshuler D. Efficiency and power in genetic association studies. Nat Genet 2005; 37:1217-23. [PMID: 16244653].

38. Malik KJ, Chen CD, Olsen TW. Stability of RNA from the retina and retinal pigment epithelium in a porcine model simulating human eye bank conditions. Invest Ophthalmol Vis Sci 2003; 44:2730-5. [PMID: 12766080].

39. Wang WH, McNatt LG, Shepard AR, Jacobson N, Nishimura DY, Stone EM, Sheffield VC, Clark AF. Optimal procedure for extracting RNA from human ocular tissues and expression profiling of the congenital glaucoma gene FOXC1 using quantitative RT-PCR. Mol Vis 2001; 7:89-94. [PMID: 11320352].

40. Komaromy AM, Petersen-Jones SM. Genetics of Canine Primary Glaucomas. Vet Clin North Am Small Anim Pract 2015; 45:1159-82. [PMID: 26277300].

41. McCarthy MI, Abecasis GR, Cardon LR, Goldstein DB, Little J, Ioannidis JP, Hirschhorn JN. Genome-wide association studies for complex traits: consensus, uncertainty and challenges. Nat Rev Genet 2008; 9:356-69. [PMID: 18398418].

42. Marchini J, Howie B, Myers S, McVean G, Donnelly P. A new multipoint method for genome-wide association studies by imputation of genotypes. Nat Genet 2007; 39:906-13. [PMID: 17572673].

43. Spencer CC, Su Z, Donnelly P, Marchini J. Designing genome-wide association studies: sample size, power, imputation, and the choice of genotyping chip. PLoS Genet 2009; 5:e1000477-[PMID: 19492015].

44. Torkamani A, Wineinger NE, Topol EJ. The personal and clinical utility of polygenic risk scores. Nat Rev Genet 2018; 19:581-90. [PMID: 29789686].

45. Utsunomiya YT, Ribeiro ÉS, Quintal AP, Sangalli JR, Gazola VR, Paula HB, Trinconi CM, Lima VM, Perri SH, Taylor JF, Schnabel RD, Sonstegard TS, Garcia JF, Nunes CM. Genome-Wide Scan for Visceral Leishmaniasis in Mixed-Breed Dogs Identifies Candidate Genes Involved in T Helper Cells and Macrophage Signaling. PLoS One 2015; 10:e0136749-[PMID: 26348501].

46. Vernau KM, Runstadler JA, Brown EA, Cameron JM, Huson HJ, Higgins RJ, Ackerley C, Sturges BK, Dickinson PJ, Puschner B, Giulivi C, Shelton GD, Robinson BH, DiMauro S, Bollen AW, Bannasch DL. Genome-wide association analysis identifies a mutation in the thiamine transporter 2 (SLC19A3) gene associated with Alaskan Husky encephalopathy. PLoS One 2013; 8:e57195-[PMID: 23469184].

47. Lindblad-Toh K, Wade CM, Mikkelsen TS, Karlsson EK, Jaffe DB, Kamal M, Clamp M, Chang JL, Kulbokas EJ 3rd, Zody MC, Mauceli E, Xie X, Breen M, Wayne RK, Ostrander EA, Ponting CP, Galibert F, Smith DR, DeJong PJ, Kirkness E, Alvarez P, Biagi T, Brockman W, Butler J, Chin CW, Cook A, Cuff J, Daly MJ, DeCaprio D, Gnerre S, Grabherr M, Kellis M, Kleber M, Bardeleben C, Goodstadt L, Heger A, Hitte C, Kim L, Koepfli KP, Parker HG, Pollinger JP, Searle SM, Sutter NB, Thomas R, Webber C, Baldwin J, Abebe A, Abouelleil A, Aftuck L, Ait-Zahra M, Aldredge T, Allen N, An P, Anderson S, Antoine C, Arachchi H, Aslam A, Ayotte L, Bachantsang P, Barry A, Bayul T, Benamara M, Berlin A, Bessette D, Blitshteyn B, Bloom T, Blye J, Boguslavskiy L, Bonnet C, Boukhgalter B, Brown A, Cahill P, Calixte N, Camarata J, Cheshatsang Y, Chu J, Citroen M, Collymore A, Cooke P, Dawoe T, Daza R, Decktor K, DeGray S, Dhargay N, Dooley K, Dooley K, Dorje P, Dorjee K, Dorris L, Duffey N, Dupes A, Egbiremolen O, Elong R, Falk J, Farina A, Faro S, Ferguson D, Ferreira P, Fisher S, FitzGerald M, Foley K, Foley C, Franke A, Friedrich D, Gage D, Garber M, Gearin G, Giannoukos G, Goode T, Goyette A, Graham J, Grandbois E, Gyaltsen K, Hafez N, Hagopian D, Hagos B, Hall J, Healy C, Hegarty R, Honan T, Horn A, Houde N, Hughes L, Hunnicutt L, Husby M, Jester B, Jones C, Kamat A, Kanga B, Kells C, Khazanovich D, Kieu AC, Kisner P, Kumar M, Lance K, Landers T, Lara M, Lee W, Leger JP, Lennon N, Leuper L, LeVine S, Liu J, Liu X, Lokyitsang Y, Lokyitsang T, Lui A, Macdonald J, Major J, Marabella R, Maru K, Matthews C, McDonough S, Mehta T, Meldrim J, Melnikov A, Meneus L, Mihalev A, Mihova T, Miller K, Mittelman R, Mlenga V, Mulrain L, Munson G, Navidi A, Naylor J, Nguyen T, Nguyen N, Nguyen C, Nguyen T, Nicol R, Norbu N, Norbu C, Novod N, Nyima T, Olandt P, O'Neill B, O'Neill K, Osman S, Oyono L, Patti C, Perrin D, Phunkhang P, Pierre F, Priest M, Rachupka A, Raghuraman S, Rameau R, Ray V, Raymond C, Rege F, Rise C, Rogers J, Rogov P, Sahalie J, Settipalli S, Sharpe T, Shea T, Sheehan M, Sherpa N, Shi J, Shih D, Sloan J, Smith C, Sparrow T, Stalker J, Stange-Thomann N, Stavropoulos S, Stone C, Stone S, Sykes S, Tchuinga P, Tenzing P, Tesfaye S, Thoulutsang D, Thoulutsang Y, Topham K, Topping I, Tsamla T, Vassiliev H, Venkataraman V, Vo A, Wangchuk T, Wangdi T, Weiand M, Wilkinson J, Wilson A, Yadav S, Yang S, Yang X, Young G, Yu Q, Zainoun J, Zembek L, Zimmer A, Lander ES. Genome sequence, comparative analysis and haplotype structure of the domestic dog. Nature 2005; 438:803-19. [PMID: 16341006].

48. Bianchi M, Dahlgren S, Massey J, Dietschi E, Kierczak M, Lund-Ziener M, Sundberg K, Thoresen SI, Kämpe O, Andersson G, Ollier WE, Hedhammar Å, Leeb T, Lindblad-Toh K, Kennedy LJ, Lingaas F, Rosengren Pielberg G. A Multi-Breed Genome-Wide Association Analysis for Canine Hypothyroidism Identifies a Shared Major Risk Locus on CFA12. PLoS One 2015; 10:e0134720-[PMID: 26261983].

49. Axenovich T, Zorkoltseva I, Belonogova N, van Koolwijk LM, Borodin P, Kirichenko A, Babenko V, Ramdas WD, Amin N, Despriet DD, Vingerling JR, Lemij HG, Oostra BA, Klaver CC, Aulchenko Y, van Duijn CM. Linkage and association analyses of glaucoma related traits in a large pedigree from a Dutch genetically isolated population. J Med Genet 2011; 48:802-9. [PMID: 22058429].

50. Lowe JK, Kukekova AV, Kirkness EF, Langlois MC, Aguirre GD, Acland GM, Ostrander EA. Linkage mapping of the primary disease locus for collie eye anomaly. Genomics 2003; 82:86-95. [PMID: 12809679].

51. Kukekova AV, Nelson J, Kuchtey RW, Lowe JK, Johnson JL, Ostrander EA, Aguirre GD, Acland GM. Linkage mapping of canine rod cone dysplasia type 2 (rcd2) to CFA7, the canine orthologue of human 1q32. Invest Ophthalmol Vis Sci 2006; 47:1210-5. [PMID: 16505060].

52. Acland GM, Ray K, Mellersh CS, Langston AA, Rine J, Ostrander EA, Aguirre GD. A novel retinal degeneration locus identified by linkage and comparative mapping of canine early retinal degeneration. Genomics 1999; 59:134-42. [PMID: 10409424].

53. van der Linde-Sipman JS. Dysplasia of the pectinate ligament and primary glaucoma in the Bouvier des Flandres dog. Vet Pathol 1987; 24:201-6. [PMID: 3603960].

54. Vandiedonck C. Genetic association of molecular traits: A help to identify causative variants in complex diseases. Clin Genet 2018; 93:520-32. [PMID: 29194587].

55. Schierding W, Cutfield WS, O'Sullivan JM. The missing story behind Genome Wide Association Studies: single nucleotide polymorphisms in gene deserts have a story to tell. Front Genet 2014; 5:39-[PMID: 24600475].

56. Huang Q. Genetic study of complex diseases in the post-GWAS era. J Genet Genomics 2015; 42:87-98. [PMID: 25819085].

57. Jiang B, Harper MM, Kecova H, Adamus G, Kardon RH, Grozdanic SD, Kuehn MH. Neuroinflammation in advanced canine glaucoma. Mol Vis 2010; 16:2092-108. [PMID: 21042562].

58. Graham KL, McCowan C, White A. Genetic and Biochemical Biomarkers in Canine Glaucoma. Vet Pathol 2017; 54:194-203. [PMID: 27681326].

59. Marshall JL, Stanfield KM, Silverman L, Khan KN. Enhanced expression of cyclooxygenase-2 in glaucomatous dog eyes. Vet Ophthalmol 2004; 7:59-62. [PMID: 14738509].

60. Pumphrey SA, Pizzirani S, Pirie CG, Anwer MS, Logvinenko T. Western blot patterns of serum autoantibodies against optic nerve antigens in dogs with goniodysgenesis-related glaucoma. Am J Vet Res 2013; 74:621-8. [PMID: 23531071].

61. Danford ID, Verkuil LD, Choi DJ, Collins DW, Gudiseva HV, Uyhazi KE, Lau MK, Kanu LN, Grant GR, Chavali VRM, O'Brien JM. Characterizing the "POAGome": A bioinformatics-driven approach to primary open-angle glaucoma. Prog Retin Eye Res 2017; 58:89-114. [PMID: 28223208].

62. Itakura T, Peters DM, Fini ME. Glaucomatous MYOC mutations activate the IL-1/NF-kappaB inflammatory stress response and the glaucoma marker SELE in trabecular meshwork cells. Mol Vis 2015; 21:1071-84. [PMID: 26396484].

63. Reilly CM, Morris R, Dubielzig RR. Canine goniodysgenesis-related glaucoma: a morphologic review of 100 cases looking at inflammation and pigment dispersion. Vet Ophthalmol 2005; 8:253-8. [PMID: 16008705].

64. Mangan BG, Al-Yahya K, Chen CT, Gionfriddo JR, Powell CC, Dubielzig RR, Ehrhart EJ, Madl JE. Retinal pigment epithelial damage, breakdown of the blood-retinal barrier, and retinal inflammation in dogs with primary glaucoma. Vet Ophthalmol 2007; 10:Suppl 1117-24. [PMID: 17973843].

65. Alario AF, Pizzirani S, Pirie CG. Histopathologic evaluation of the anterior segment of eyes enucleated due to glaucoma secondary to primary lens displacement in 13 canine globes. Vet Ophthalmol 2013; 16:Suppl 134-41. [PMID: 22498049].

Articles are provided courtesy of Emory University and the Zhongshan Ophthalmic Center, Sun Yat-sen University, P.R. China. The print version of this article was created on 8 February 2019. This reflects all typographical corrections and errata to the article through that date. Details of any changes may be found in the online version of the article.